AMMRC TR 76-9

FRACTURE OF COMPOSITE COMPACT TENSION SPECIMENS

JOHN M. SLEPETZ and LEONARD CARLSON
MECHANICS OF MATERIALS DIVISION

March 1976

ARMY MATERIALS AND MECHANICS RESEARCH CENTER
Watertown, Massachusetts 02172

The findings in this report are not to be construed as an official Department of the Army position, unless so designated by other authorized documents.

Mention of any trade names or manufacturers in this report shall not be construed as advertising nor as an official indorsement or approval of such products or companies by the United States Government.

DISPOSITION INSTRUCTIONS

When this report is no longer needed, Department of the Army organizations will destroy it in accordance with the procedures given in AR 380-5. Navy and Air Force elements will destroy it in accordance with applicable directions. Department of Defense contractors will destroy the report according to the requirements of Section 14 of the Industrial Security Manual for Safeguarding Classified Information. All others will return the report to Army Materials and Mechanics Research Center.

UNCLASSIFIED

SECURITY CLASSIFICATION OF THIS PAGE (When Date Entered)

REPORT DOCUMENTATION PAGE		READ INSTRUCTIONS BEFORE COMPLETING FORM
1. REPORT NUMBER AMMRC TR 76-9	2. GOVT ACCESSION NO.	3. RECIPIENT'S CATALOG NUMBER
4. TITLE (and Subtitle) FRACTURE OF COMPOSITE COMPACT TENSION SPECIMENS		5. TYPE OF REPORT & PERIOD COVERED 6. PERFORMING ORG. REPORT NUMBER
7. AUTHOR(s) John M. Slepetz and Leonard Carlson		8. CONTRACT OR GRANT NUMBER(s)
9. PERFORMING ORGANIZATION NAME AND ADDRESS Army Materials and Mechanics Research Center Watertown, Massachusetts 02172 DRXMR-TM		10. PROGRAM ELEMENT, PROJECT, TASK AREA & WORK UNIT NUMBERS D/A Project: 1T162105AH84 AMCMS Code: 612105.11.H8400 Agency Accession: DA 0C4687
11. CONTROLLING OFFICE NAME AND ADDRESS U. S. Army Materiel Development and Readiness Command, Alexandria, Virginia 22333		12. REPORT DATE March 1976 13. NUMBER OF PAGES 22
14. MONITORING AGENCY NAME & ADDRESS(if different from Controlling Office)		15. SECURITY CLASS. (of this report) Unclassified 15a. DECLASSIFICATION/DOWNGRADING SCHEDULE

16. DISTRIBUTION STATEMENT (of this Report)

Approved for public release; distribution unlimited.

17. DISTRIBUTION STATEMENT (of the abstract entered in Block 20, if different from Report)

18. SUPPLEMENTARY NOTES

Presented at the ASTM Symposium on Fracture of Composites, September 1974; final paper published in ASTM STP 593, November 1975.

19. KEY WORDS (Continue on reverse side if necessary and identify by block number)

Composite materials	Crack propagation
Fiber composites	Mechanical properties
Fracture (materials)	Test methods

20. ABSTRACT (Continue on reverse side if necessary and identify by block number)

(SEE REVERSE SIDE)

DD FORM 1 JAN 73 1473 EDITION OF 1 NOV 65 IS OBSOLETE

UNCLASSIFIED

SECURITY CLASSIFICATION OF THIS PAGE (When Date Entered)

Block No. 20

ABSTRACT

Fracture experiments were carried out on compact tension specimens of unidirectional and cross-ply S-glass/epoxy and graphite/epoxy. Fracture toughness values were determined by the compliance calibration technique and by measuring the area under the load-displacement curve. In unidirectional specimens, crack extension was always parallel to the fibers and was dependent on crack length. Toughness did not vary significantly with fiber orientation relative to the load direction in unidirectional S-glass/epoxy. Tests on cross-ply S-glass specimens were not valid because crack propagation did not occur; instead, a zone containing a system of superficial parallel cracks and other damage developed, which extended with increasing load. Cross-ply graphite specimens, on the other hand, did appear to give valid test results although the cracks propagated were not always straight and other damage mechanisms were also present. Toughness values for cross-ply graphite were approximately two orders of magnitude higher than for unidirectional specimens due chiefly to the fracture resistance of fibers transverse to the crack. Toughness values determined by the compliance calibration method were consistent with reported values obtained by other methods.

Authorized Reprint from
Special Technical Publication 593

American Society for Testing and Materials
1916 Race Street, Philadelphia, Pa. 19103
1975

J. M. Slepetz[1] *and L. Carlson*[1]

Fracture of Composite Compact Tension Specimens

REFERENCE: Slepetz, J. M. and Carlson, L., "**Fracture of Composite Compact Tension Specimens,**" *Fracture Mechanics of Composites, ASTM STP 593,* American Society for Testing and Materials, 1975, pp. 143–162.

ABSTRACT: Fracture experiments were carried out on compact tension specimens of unidirectional and cross-ply S-glass/epoxy and graphite/epoxy. Fracture toughness values were determined by the compliance calibration technique and by measuring the area under the load-displacement curve. In unidirectional specimens, crack extension was always parallel to the fibers and was dependent on crack length. Toughness did not vary significantly with fiber orientation relative to the load direction in unidirectional S-glass/epoxy. Tests on cross-ply S-glass specimens were not valid because crack propagation did not occur; instead, a zone containing a system of superficial parallel cracks and other damage developed, which extended with increasing load. Cross-ply graphite specimens, on the other hand, did appear to give valid test results although the cracks propagated were not always straight and other damage mechanisms were also present. Toughness values for cross-ply graphite were approximately two orders of magnitude higher than for unidirectional specimens due chiefly to the fracture resistance of fibers transverse to the crack. Toughness values determined by the compliance calibration method were consistent with reported values obtained by other methods.

KEY WORDS: fracture properties, composite materials, fractures (materials), crack propagation, mechanical properties, fiber composites, evaluation, tests

The prediction of failure in fiber reinforced composites having geometric discontinuities or inherent material defects is perplexing due to the complex fracture mechanisms which are characteristic of heterogeneous materials. Linear elastic fracture mechanics has been applied to failure phenomena in composites with some success [*1–5*][2] despite the difference in behavior from homogeneous materials. The use of fracture mechanics to predict failure is based on the existence of a material property, fracture toughness, defined by either the critical stress intensity factor, K_c, or critical strain energy release rate, G_c. These two properties are equivalent,

[1] Civil engineer and research assistant, respectively, Army Materials and Mechanics Research Center, Watertown, Mass. 02172.

[2] The italic numbers in brackets refer to the list of references appended to this paper.

being related through the elastic constants of the material [6]. The relationship between stress intensity factor, K, and strain energy release rate, G, for an orthotropic material in the crack opening mode is

$$G = K^2 \left(\frac{A_{11}A_{22}}{2}\right)^{1/2} \left[\frac{A_{22}}{A_{11}} + \frac{2A_{12} + A_{66}}{2A_{11}}\right]^{1/2} \tag{1}$$

A_{11}, A_{12}, etc. are the elastic compliances associated with the principal material directions. G_c is defined as the value of G at which unstable crack growth occurs.

G can be determined experimentally by compliance calibration of compact tension specimens. The relatively high load point displacements obtained with this type of specimen make it well suited to the compliance calibration technique. Also, under fixed grip conditions, crack growth is inherently stable in the compact tension specimen. Because G decreases with crack length, a crack which propagates at an instability load is generally arrested after a short growth interval. Consequently, a number of toughness measurements can be made on a single specimen [7]. The dependence of toughness on crack length and the development of various fracture mechanisms can be studied more closely since the failure process is controlled.

Most of the work in fracture of composites has been conducted on specimens other than the compact tension type. The applicability of linear elastic fracture mechanics to unidirectional composites in which the crack direction is predetermined to be parallel to the fibers was established in early studies by Wu [1,2] and extended by Lauraitis [3]. Wu developed an interaction relationship for combined Mode I and Mode II fracture using primarily center-notched tension specimens in the experiments. Lauraitis proposed a composite failure criterion based on the existence of inherent microcracks with the critical strain energy release rate, G_c, as the basic strength parameter. Unnotched tension specimens were used to verify the criterion. The extension of fracture mechanics to angle-ply and cross-ply materials has been less satisfactory because cracks do not always propagate in a direction of material symmetry as in unidirectional composites and because more complex damage phenomena such as delamination between plies and splitting within plies occur. Fracture of cross-ply composites has been studied using center or edge-notched tension specimens [4,5,8] and notched bend specimens [4,8]. The present study utilizes compact tension specimens to investigate fracture behavior in unidirectional and cross-ply composites. The main objectives are to identify the failure processes which occur in both types of laminates, determine the critical strain energy release rate, G_c, and evaluate the suitability of a fracture mechanics approach to cross-ply composites.

Experimental Procedures

Materials and Specimens

The compact tension specimens were machined from laminate panels of S-glass or graphite/epoxy which had been fabricated commercially by a tape lay-up and autoclave cure process. The S-glass panels were 1002S Scotchply,[3] 12 plies thick; and the graphite laminates were Modulite[4] 5208, eight plies thick. Both high modulus graphite (MOD I) and high strength graphite (MOD II) panels were tested. The laminates were fabricated with all unidirectional plies or with a balanced and symmetric cross-ply configuration having equal numbers of plies in two orthogonal directions. The elastic properties of test materials were determined by tension and shear tests on coupon specimens and are given in Table I along with the nominal volume fraction of fibers in the cured laminate.

TABLE 1—*Laminate properties.*

Material	E_1	E_2	G_{12}	μ_{12}	Fiber Volume, %
	lb/in.^{2} × 10^6				
1002 S-glass/epoxy					
Unidirectional	6.9	2.3	1.0	0.28	55
Crossply	4.7	4.7	1.1	0.14	
MOD I-5208 graphite/epoxy					
Unidirectional	19.9	1.11	0.93	0.32	40
Crossply	12.0	12.0	0.93	0.021	
MOD II-5208 graphite/epoxy					
Unidirectional	19.5	0.96	1.02	0.32	60
Crossply	12.1	12.1	0.95	0.035	

The compact tension specimen configuration used in most of the fracture experiments is shown in Fig. 1. In unidirectional S-glass/epoxy specimens the fiber direction with respect to the load direction was a test parameter, the various orientations being 0°, 30°, 45°, 60°, and 90°. Tests on unidirectional graphite specimens were conducted only with 0° or 90° fiber orientation. Cross-ply specimens of both S-glass and graphite were tested with the outer plies oriented at 0°, 45°, or 90° with respect to the applied load. It was necessary to constrain the cross-ply specimens to prevent out-of-plane bending. This was accomplished by clamping 0.125 in. thick lubricated steel plates to both sides of the specimen. The specimen in-plane compliance was unaffected, but out-of-plane deformation was satisfactorily limited. The test plan employed in the study is given in Table 2.

[3] Trade name, 3M Company.
[4] Trade name, Whittaker Division of NARMCO.

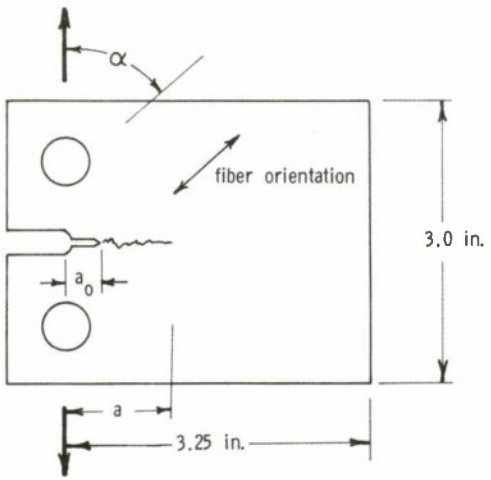

FIG. 1—*Compact tension specimen configuration.*

Compliance Test Procedure

Fracture toughness, characterized by the critical strain energy release rate, was determined using the compliance calibration technique. The compact tension specimens were loaded in an approximately fixed grip mode at a cross-head speed of 0.01 in./min. Load point displacement was measured by means of a clip gage. Displacement, together with applied load, were plotted on an X-Y recorder. The usual procedure followed was to load the specimen until an increment of crack propagated from the machined notch. Under the test grip conditions the load decreased sharply when this occurred and the crack was arrested. The new crack length was measured and the specimen was unloaded and reloaded to determine the change in compliance. The procedure was repeated a number of times until the crack had propagated to about 80 percent of the specimen width. A least squares curve fit was made to the experimental compliance calibration versus crack length relationship. The function found to best fit the compliance data over the widest range of crack lengths was

$$C = A_1(a/w) + A_2(a/w)^3 + A_3 \frac{2 + a/w}{(1 - a/w)^2} \tag{2}$$

in which C is compliance, a is crack length, and w is specimen width measured from the load line. A_1, A_2, and A_3 are the constants determined from the least squares fit. It can be seen that the three terms on the right side of Eq 2 qualitatively represent the compliance contributions due to beam shear, bending, and net section stress, respectively, in the compact tension specimen.

For an elastic body with an incrementally growing crack the strain energy release rate, G, can be determined experimentally from Ref 6.

$$G = \frac{F^2}{2t} \frac{dC}{da} \tag{3}$$

where F is the applied load, t is specimen thickness, and dC/da is the derivative of compliance with respect to crack length obtained from the experimental compliance curve, Eq 2. In this study, G_c was defined as the value G at which a crack in the specimen begins to grow unstably before being arrested. This occurs at a load, F_c, taken as the maximum load in the cycle of crack growth.

Fracture Work Procedure

In addition to the compliance technique the average fracture energy was determined by measuring the area under the load-displacement curve during an interval of crack extension. Under quasi-static loading conditions this method provided a rough check on the results obtained by compliance calibration; however, the latter is predicated on elastic behavior while the total fracture energy under the load curve would include any energy

TABLE 2—*Test plan.*

Laminate	α	No. of Tests	Initial Notch Length
1002 S-glass/epoxy			
Unidirectional	0	4	3/8
	90	12	3/8
	30	4	3/8
	45	4	3/8
	60	4	3/8
Crossply	0	4	3/4
	90	4	3/4
	45	2	3/4
MOD I graphite/epoxy			
Unidirectional	0	4	3/8
	90	4	3/8
Crossply	0	2	3/4
	9	2	3/4
	45	4	3/4
MOD II graphite/epoxy			
Unidirectional	0	4	3/8
	90	4	3/8
Crossply	0	8	3/4
	90	8	3/4
	45	4	3/4

dissipated by nonconservative behavior such as plastic deformation. An elastic finite element analysis of the compact tension specimen was undertaken to obtain an estimate of the variation of compliance with crack length. Plane stress orthotropic elements were used having the elastic properties given in Table 1 for the respective materials employed in the study. This was done to determine the suitability of using analytical rather than experimental calibration procedures as is commonly done with metal compact tension specimens.

Experimental Results

Unidirectional Specimens

Crack extension occurred parallel to the fibers in unidirectional compact tension specimens regardless of load orientation. This preferred crack orientation has previously been observed in other types of specimen [*1,3,8*] and causes some difficulty in data interpretation. Except for the case $\alpha = 90°$, crack growth along the fiber direction occurs by a combination of crack opening and forward shear fracture modes (Mode I and Mode II, respectively). The energy contributions of each mode are not experimentally separable by the compliance technique. Only when $\alpha = 90°$ would crack growth be expected to be by Mode I fracture only. In principle, the compliance technique is not limited to measuring G for Mode I fracture [*6,9*]; however, experimental difficulties in obtaining the compliance derivative of Eq 3 accurately for the inclined crack and specimen geometry employed make the application questionable. The work of fracture, W_f, measured by the area under the load-displacement curve also comprises the contributions of both modes. W_f was used instead of G_c to investigate the variation of fracture energy with fiber orientation in unidirectional S-glass specimens.

The load-displacement behavior of S-glass and graphite specimens was essentially linear until the onset of incremental crack growth. This is seen in Fig. 2 which shows the successive load displacement curves obtained for a unidirectional MOD II specimen with $\alpha = 90°$. For clarity the unloading curves are not shown. The compliance curves for MOD I and MOD II specimens appear in Fig. 3 with the finite-element values shown as the dashed line. The latter predictions are significantly higher than measured compliances except for small crack lengths. Crack growth in graphite specimens occurred typically by short pop-in bursts accompanied by a sharp decrease in load as seen in Fig. 2. With S-glass specimens, however, crack growth occurred by slow tearing, giving the load-deformation curve a rounded appearance at the top of the load cycle instead of the sharp peaks observed with graphite specimens. In addition to matrix

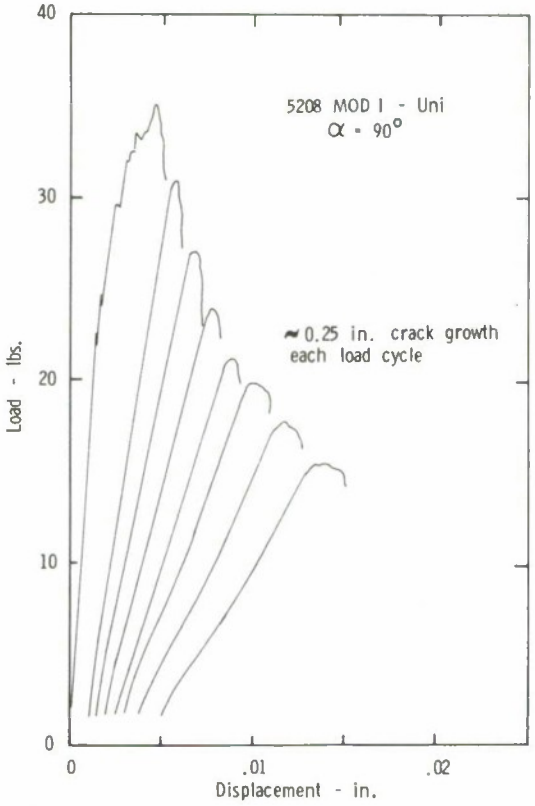

FIG. 2—*Load-displacement history for a unidirectional MOD I graphite/epoxy specimen.*

crack propagation all unidirectional specimens, but especially S-glass specimens, exhibited some degree of fiber bridging behind the advancing crack tip. This phenomenom is pictured in Fig. 4*a* which shows the network of fibers being pulled across the crack surface well behind the crack tip. In Fig. 4*b* these fibers are shown after the crack has completely penetrated the specimen. This fiber bridging action tends to increase both the specimen stiffness and toughness. The relative effect of this action was studied by machining away these fibers after each cycle of crack growth in tests on several S-glass specimens. The compliance curves obtained for natural and machined cracks are shown in Fig. 5 along with the finite element values represented by the dashed line. The compliance values for the machined notch (solid data points) were the highest observed; and the finite element predicted values were intermediate to those of the machined and natural crack values.

The fracture toughness, G_c, of S-glass specimens is shown as a function of normalized crack length in Fig. 6. The values obtained for specimens

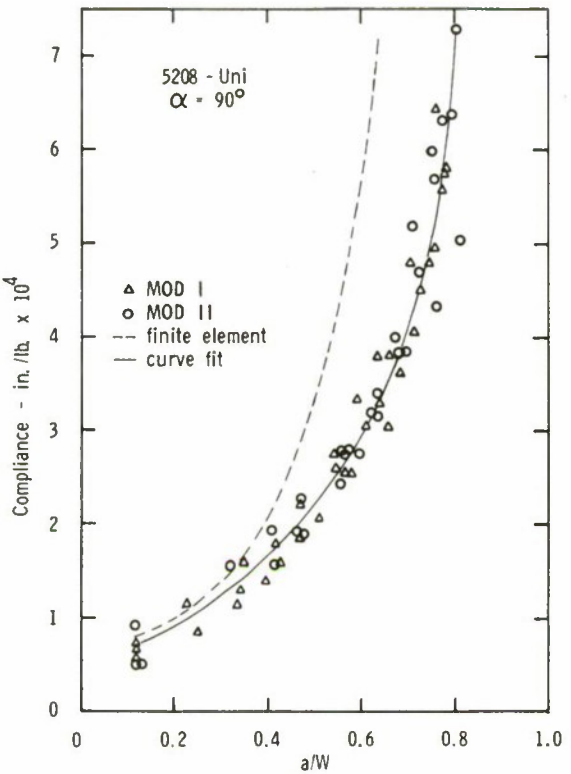

FIG. 3—*Compliance versus crack length curves for MOD I and MOD II specimens.*

with natural cracks showed a dependence on crack length up to about 30 percent of the specimen width, after which G_c leveled off at a mean value of 7.6 lb/in. The dependence on crack length can be attributed to the development of the fiber bridging action just discussed. In the case of the machined crack, on the other hand, G_c was essentially independent of crack length with a mean value of 3.2 lb/in., which is about the same as reported values for the epoxy matrix alone [*8*]. From the observed difference in G_c between the natural and machined crack tests, the fiber bridging action can be seen to contribute significantly to fracture toughness parallel to the fibers of unidirectional S-glass composites. Toughness values for MOD I and MOD II graphite specimens were much lower than those of the S-glass specimens with natural cracks. The mean values of G_c obtained (see Fig. 7) were 2.30 and 1.88 lb/in. for MOD I and MOD II, respectively. Significantly, there appeared to be much less fiber bridging than with S-glass specimens, perhaps due to the higher stiffness of graphite fibers. Table 3 summarizes the mean fracture toughness results for all unidirectional specimens tested at $\alpha = 90°$. Also

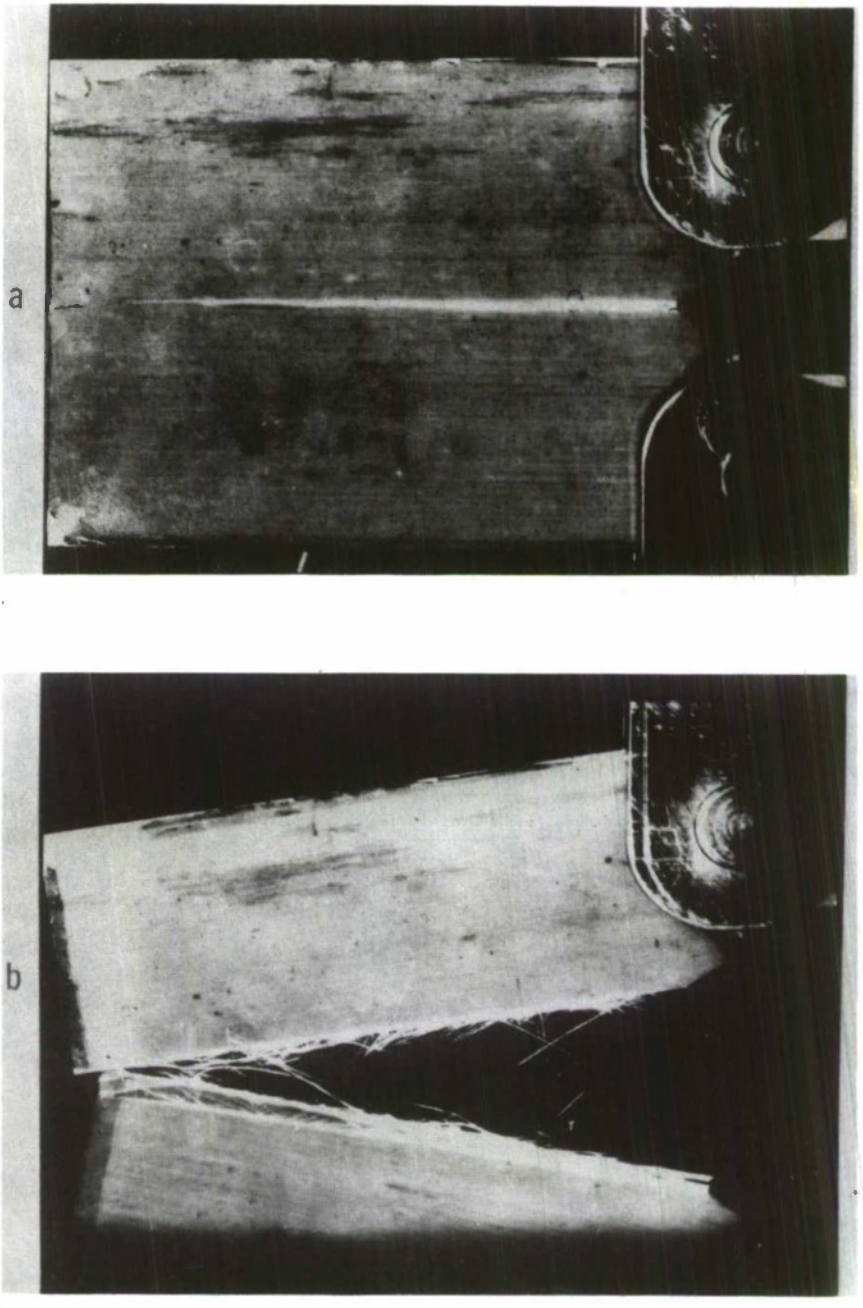

FIG. 4—*Fiber bridging action in a unidirectional S-glass/epoxy specimen,* (a) *with crack length at 0.8 W,* (b) *after complete fracture.*

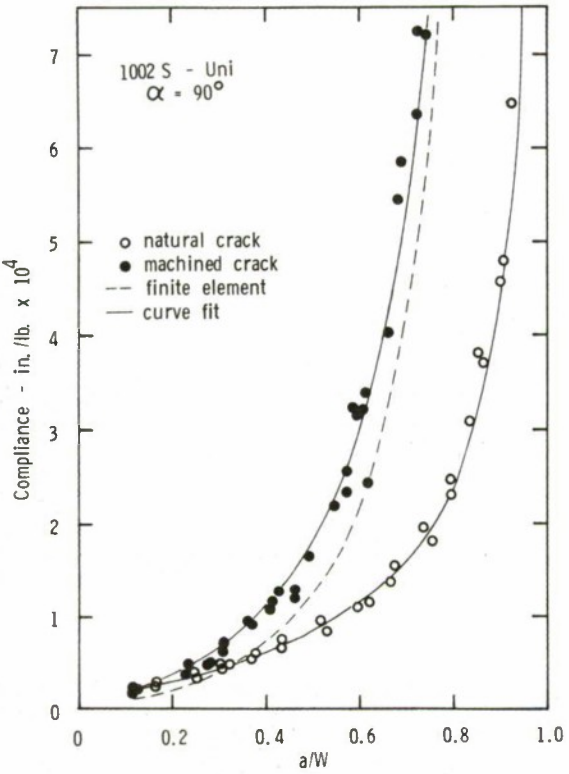

FIG. 5—*Compliance versus crack length curves for S-glass/epoxy specimens with machined and natural cracks.*

given in the table are the work of fracture values obtained from the area under the load-displacement curve and designated as W_f. There was reasonably good agreement between W_f and G_c, the latter tending to be slightly higher. In all fracture toughness tests conducted, there was considerable data scatter. The standard deviation of G_c ranged from 11 to 25 percent of the mean value. Variation within a single specimen was often greater than between two different specimens of the same material.

TABLE 3—*Mean fracture toughness values, unidirectional specimens (α = 90°).*

Material	G_c, lb/in.	W_f, lb/in.
S-glass/epoxy		
Natural crack	7.65	7.27
Machined crack	3.18	...
MOD I graphite/epoxy	2.30	1.97
MOD II graphite/epoxy	1.88	1.74

The work of fracture values were used to determine the effect of fiber orientation on toughness in S-glass specimens. In Fig. 8 these data are plotted against inclined crack length measured from the initial notch. In this plot are data from specimens of all the various fiber orientations. These plot roughly as a straight line corresponding to W_f = 6.85 lb/in., and no distinction can be made among the data on the basis of fiber orientation. Within the data spread there does not appear to be a variation in toughness with fiber orientation. This supports the hypothesis offered in Ref *3* that

$$G_c = G_I + G_{II} = \text{Constant} \tag{4}$$

for unidirectional composites in which crack propagation is parallel to fibers. G_I and G_{II} are the strain energy release rates in the crack opening and forward shear modes, respectively. The crack direction is predetermined by fiber orientation, and the relative contributions of G_I and G_{II} are fixed by this orientation and possibly by crack length; but the sum of the separate contributions of the two modes remains a material constant with crack extension.

One further observation was made in the unidirectional specimen tests. It was impossible to measure G_c for specimens with $\alpha = 0$ as one of the

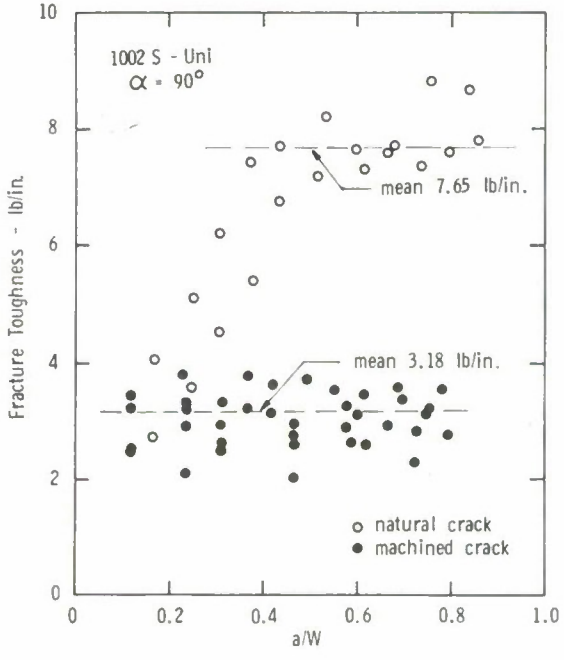

FIG. 6—*Variation of fracture toughness,* G_c, *with crack length in unidirectional S-glass/epoxy specimens.*

arms in the double cantilever region generally broke off because of the tendency for the crack to travel parallel to the fibers. Several attempts were made to propagate the crack across fibers in specimens of this orientation by bonding doublers to them in order to prevent crack growth parallel to the fibers. These attempts were unsuccessful and the only successful method found to propagate a crack across the fibers was to machine a deep side groove in a cross-ply specimen such that only two plies of the 8-ply laminate remained. Those two remaining plies were normal to plane of the crack. This method worked only with graphite specimens. G_c values based on the reduced thickness in the groove were obtained for two MOD II specimens and are shown in Fig. 7. The mean value observed was 355 lb/in., more than two orders of magnitude higher than for specimens with $\alpha = 90°$.

Cross-Ply Specimens

Not only was the behavior of cross-ply fracture specimens different from that of unidirectional specimens, but there was a marked difference in behavior between S-glass and graphite cross-ply specimens. In S-glass

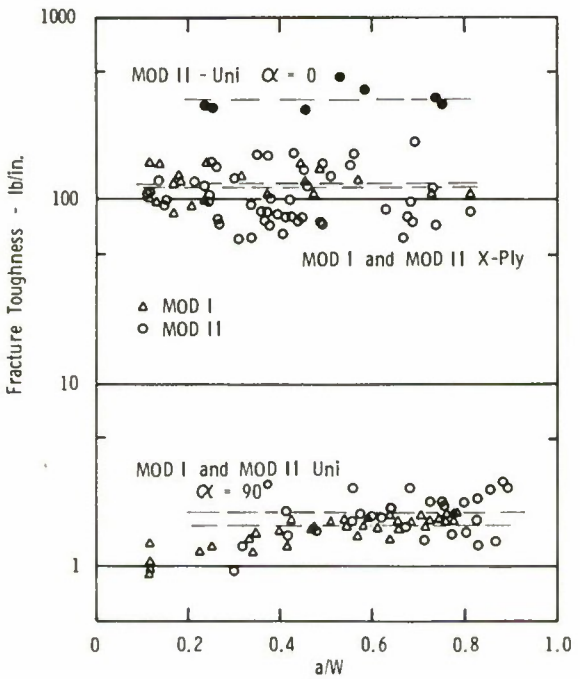

FIG. 7—*Variation of fracture toughness,* G_c, *with crack length in unidirectional and cross-ply graphite/epoxy specimens.*

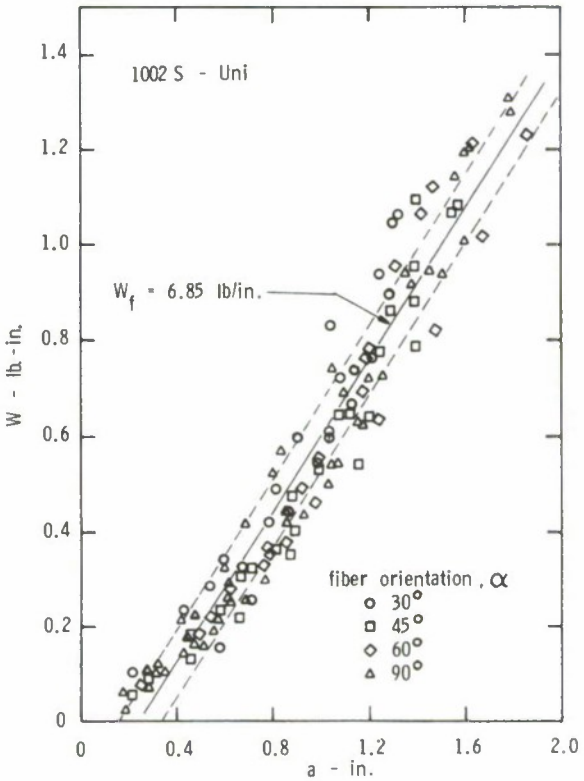

FIG. 8—*Work of fracture versus crack length in unidirectional S-glass/epoxy specimens having various fiber orientations.*

specimens some early cracking occurred at the notch tip at loads comparable to those at initial cracking in unidirectional specimens. After this, a system of superficial cracks parallel to the fibers in the various plies developed, and the load-displacement behavior became nonlinear in a way usually characteristic of gross plastic deformation. The damage zone was considerably larger than the plastic zone ahead of the crack tip in a metal specimen and tended to dominate subsequent behavior. Figure 9 shows such a zone developing in a specimen with the outer plies oriented at 45° to the load. In Fig. 9*a* the first crack is seen at the notch tip, having occurred at a load of about 170 lb. The photograph was taken subsequently at a load of 800 lb. A dye penetrant was used to improve contrast between the crack and specimen surface. In Fig. 9*b* the load has been increased to 1300 lb; but the initial crack has not extended; instead, the system of parallel, one-ply thickness cracks has developed. The corresponding load-displacement curve during this cracking sequence is seen in Fig. 10. Generally, this damage zone continued to spread with further

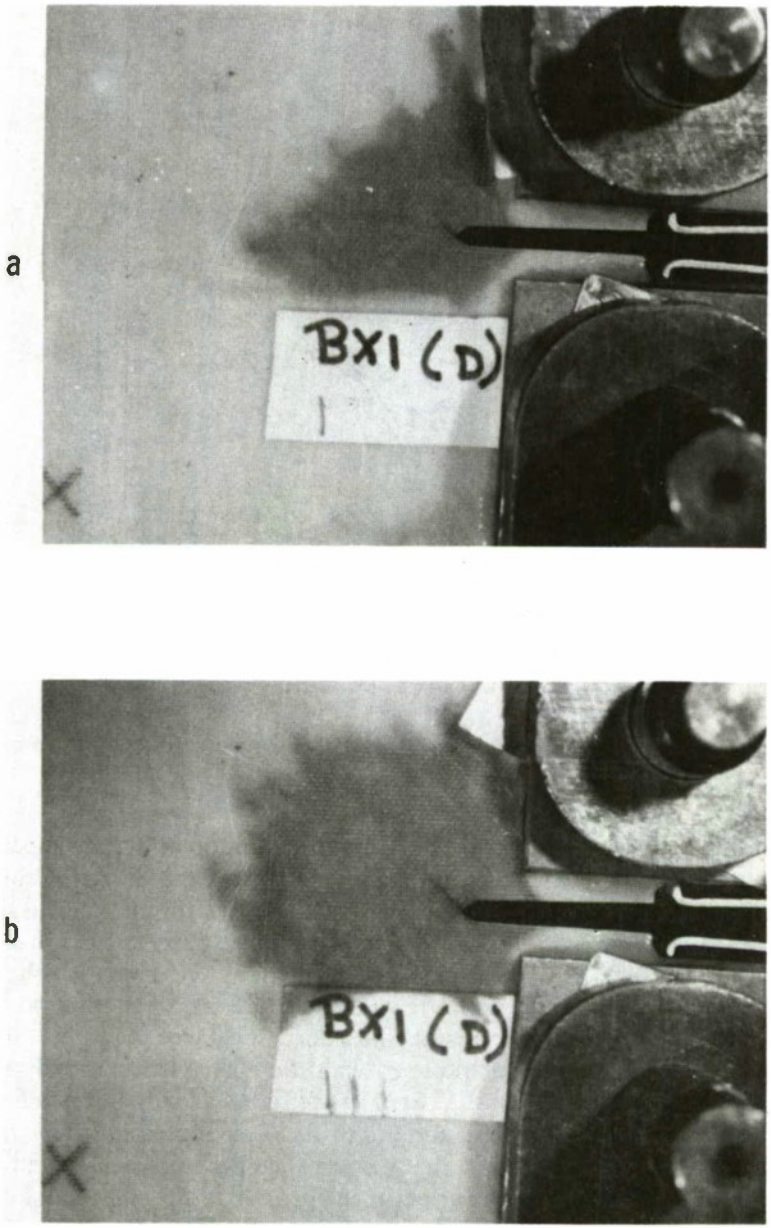

FIG. 9—(a) *Initial crack in a cross-ply S-glass/epoxy specimen* ($\alpha = 45°$); (b) *System of parallel, one-ply deep cracks at increased load.*

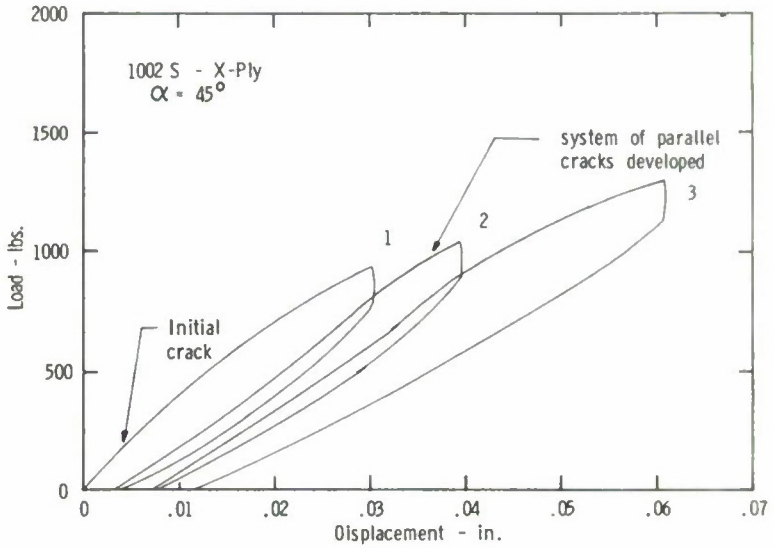

FIG. 10—*Load-displacement history for cross-ply of an S-glass/epoxy specimen.*

load increase without development and extension of a through crack. Since there was no crack propagation, no determination of G_c could be made for the S-glass/epoxy cross-ply specimens. The type of damage mechanism observed suggests that the usual fracture mechanics approach is inappropriate for these materials. The development of an alternative procedure would require a way of quantitatively evaluating the extent of the damage zone throughout the various plies.

The cross-ply MOD I and MOD II specimens behaved in a more brittle fashion than the S-glass/epoxy specimens. In general, a sharp crack was propagated from the notch; however, crack extension with increased load was frequently in a zig-zag direction, parallel at any time to one or the other ply directions. This is seen in Fig. 11*a* and *b* which show the crack at two different stages of development in a cross-ply MOD II specimen with a 45° orientation. Other damage mechanisms such as fiber debonding, ply delamination, and periodic splitting ahead of the crack in plies parallel to the load direction were also frequently observed. The load-deformation behavior was essentially linear even after damage occurred. The splitting observed occurred in tests in which the outer specimen plies were parallel to the load. Cracks in the outer plies occurred at regular intervals and were perpendicular to the main crack and usually accompanied by local delamination. In specimens with the outer plies perpendicular to the load such splitting occurred to a much lesser degree in the inner parallel plies due to constraint from the outer plies. The effect of the

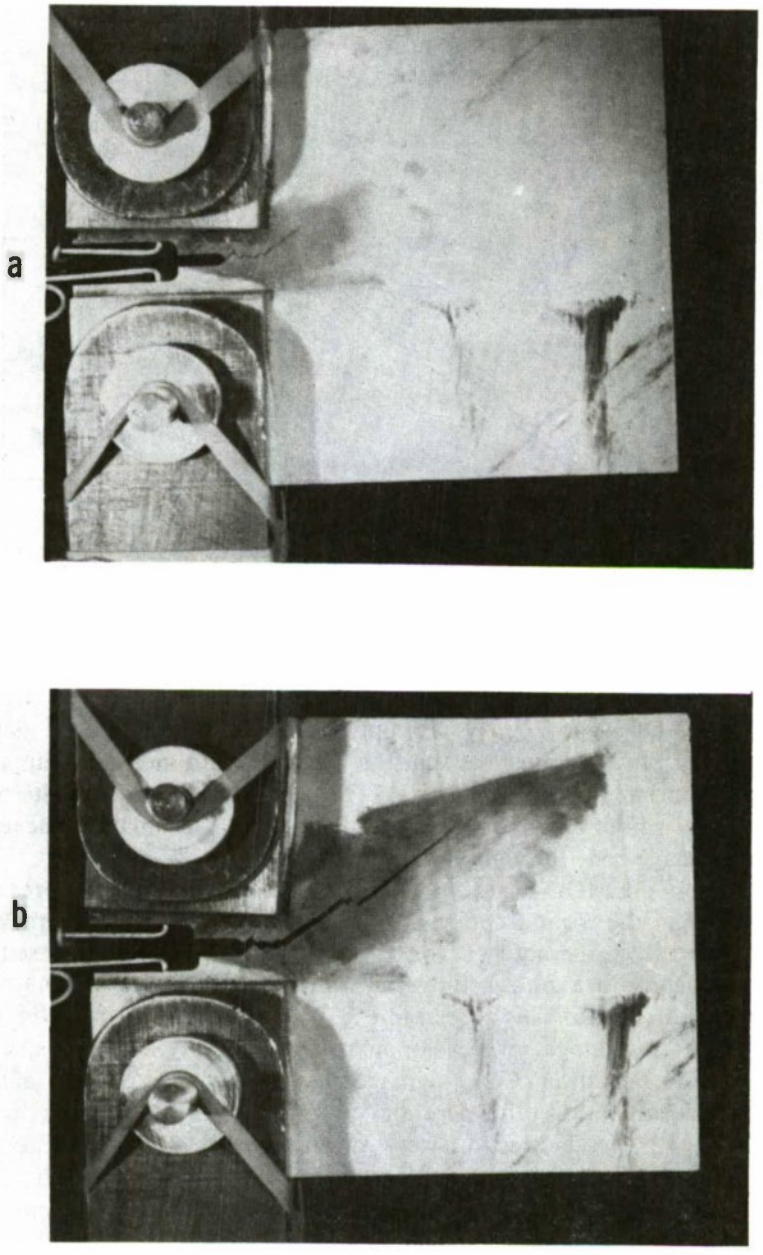

FIG. 11—*Crack development in a cross-ply graphite/epoxy specimen (α = 45°) at two different stages of loading.*

splitting was found to increase the overall specimen compliance, but there was no significant effect on the measured fracture toughness.

Figure 12 shows the compliance curves based on data for all MOD I and MOD II specimens. The finite element solution is shown as the dashed line; and in contrast to the case of unidirectional specimens, it predicts lower compliance values with crack length than were observed experimentally. This discrepancy may be due to the splitting and delamination in plies parallel to the load. In general, the finite-element predictions for all specimen types varied too widely from experimental compliance values to be used as an alternative calibration procedure. A reexamination of the finite-element model may be required to obtain compliance predictions more in line with observed values. Figure 7 shows the fracture toughness, G_c, as a function of crack length for all MOD I and MOD II specimens except those at $\alpha = 45°$ to be discussed later.

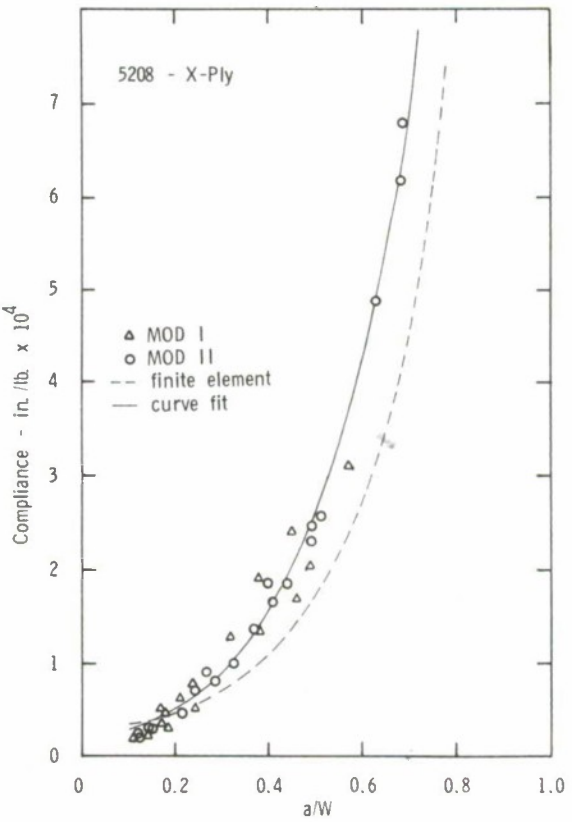

FIG. 12—*Compliance versus crack length curves for MOD I and MOD II cross-ply specimens ($\alpha = 0$ and 90°).*

The mean value of G_c was 124 lb/in. for MOD I and 117 lb/in. for MOD II cross-ply specimens. There was no apparent dependence of G_c on crack length in either case. As with unidirectional specimens, there was wide data scatter, the standard deviation being about 15 percent of the mean. The variation was evident within a single specimen as well as from specimen to specimen and may be attributable to the random interaction of secondary failure modes discussed previously with the propagating crack. Another factor could be the random variation of fiber strength within the laminate.

The test results for the three types of MOD II specimens given in Fig. 7 indicate that the principal source of toughness in graphite composites is fracture across the fibers. G_c for unidirectional specimens with $\alpha = 0$ was about three times that for cross-ply specimens. Referring to Eq 1 to relate G to K at fracture in orthotropic laminates, and using the respective elastic properties in Table 1 for unidirectional and cross-ply graphite results in a mean value of K_c of 27.0 lb/in.$^2\sqrt{\text{in.}}$ for cross-ply specimens and 51.3 lb/in.$^2\sqrt{\text{in.}}$ for unidirectional specimens. The latter value is about twice that of the cross-ply laminate, which indicates that the stress intensity at fracture is nearly the same in the cross-ply laminate as in the unidirectional laminate. Fracture of plies at $\alpha = 90°$, delamination, and splitting in plies at $\alpha = 0$ would seem to contribute negligibly to overall fracture resistance of cross-ply specimens. On the other hand, fiber debonding and pull-out in plies at $\alpha = 0$ might be expected to make a significant contribution since these are mechanisms associated with fracture across fibers in graphite composites [*4,8*]. The mean work of fracture, W_f was found from the load-deformation curves to be 121 and 107 lb/in. for MOD I and MOD II cross-ply, respectively. These values agree well with the G_c values obtained by compliance calibration. In the case of cross-ply specimens oriented at 45° to the load direction, the compliance technique was not applicable for reasons previously discussed, but W_f was found to be 91 lb/in. for MOD I and 67 lb/in. for MOD II cross-ply. Thus, the work of fracture of cross-ply laminates, unlike the unidirectional case, varies with orientation with respect to the load.

The results obtained on graphite composites in this study have been compared with results obtained using other types of specimens in Table 4. The reference test methods cited use center-notched, slow bend, and tapered double-cantilever specimens. In the first of these, G_c was determined indirectly from K_c through Eq 1. In the slow bend test G_c was obtained from the area under the load-displacement curve. In general, the G_c values of this study compare well with center-notched specimen data for both MOD I and MOD II cross-ply graphite; but the W_f values are widely different from the slow-bend test results. The valid application of compact tension specimens to fracture characterization of composites is subject to the requirement that K_c and G_c are related through the elastic constants.

TABLE 4—*Fracture test results for graphite/epoxy.*

Material	G_c,* lb/in.	W_f,* lb/in.	G_c, lb/in.	Test Method (Ref)
Mod I (40% V_f)				
Unidirectional	2.3	2.0	2.9	center notched [8]
			3.0	slow bend [8]
Crossply	124	121	117	center notched [4]
			153	slow bend [4]
MOD II (60% V_f)				
Unidirectional	1.9	1.7	...	
Crossply	117	107	110	tapered DCB [4]
			115	center notched [4]
			68	slow bend [4]

*This study.

While there is wide data scatter and secondary fracture mechanisms are present in addition to crack propagation, this requirement appears to be reasonably well satisfied in the case of cross-ply graphite specimens.

Conclusions and Discussion

The compact tension fracture test gave valid results for unidirectional composite specimens with orientations other than $\alpha = 0$; however, the compliance calibration technique with this specimen is limited by practical consideration to $\alpha = 90°$. The test also gave valid results for graphite/epoxy cross-ply composites. It does not seem that the test method is applicable to cross-ply or angle-ply S-glass/epoxy composites because of the complex failure zone which develops in lieu of a sharp crack.

In unidirectional specimens, fracture toughness is dependent on crack length in the early stages of crack growth due to the development of the network of fibers bridging the crack plane behind the advancing tip. At certain crack lengths this network becomes fully effective and toughness remains constant with additional crack growth. This mechanism contributes a significant portion of the overall toughness of unidirectional composites, more so in S-glass/epoxy than in graphite/epoxy composites. The toughness of unidirectional composites is comparatively small as a result of the tendency for cracks to propagate parallel to, rather than across, fibers regardless of load orientation.

Cross-ply graphite specimens do not exhibit a dependence of toughness on crack length. Toughness values have considerable scatter from point to point within a given specimen due to random processes occurring in addition to crack propagation and due to material property variation. G_c values obtained from compact tension specimens of cross-ply graphite are reasonably consistent with K_c values determined by

other test methods. This may be only a fortuitous coincidence in view of the complex failure behavior, and additional work is needed on various laminate configurations and stacking sequences before the application of linear elastic fracture mechanics to failure prediction of graphite composites is fully justified.

Acknowledgments

The authors gratefully acknowledge the assistance of Colin Freese of The Army Materials and Mechanics Research Center in developing the compliance curve fit program and of Agnes Travers in typing the manuscript.

References

[1] Wu, E. M. and Reuter, R. C., "Crack Extension in Fiberglass Reinforced Plastics," University of Illinois T and AM, Report No. 275, 1965.

[2] Wu, E. M., "Fracture Mechanics of Anisotropic Plates," *Composite Materials Work Shop*, Vol. I, Technomic, 1968.

[3] Lauraitis, K., "Tensile Strength of Off-Axis Unidirectional Composites," University of Illinois T and AM, Report No. 344, 1971.

[4] Phillips, D. C., "Fracture Mechanics of Carbon Fibre Laminates," *Journal of Composite Materials*, Vol. 8, April 1974.

[5] Mandell, J. F. et al, "Fracture of Graphite Fiber Reinforced Composites," Technical Report AFML-TR-73-142, July 1973.

[6] Paris, P. C. and Sih, G. C. in *Fracture Toughness Testing, ASTM STP 381*, American Society for Testing and Materials, 1970, pp. 30–83.

[7] Mostovoy et al in *Journal of Materials*, Vol. 2, No. 3, 1967, pp. 661–681.

[8] Beaumont, P. W. R. and Harris, R., "The Energy of Crack Propagation in Carbon Fibre-Reinforced Resin Systems," *Journal of Materials Science*, Nov. 1972.

[9] Bueckner, H. F., "The Propagation of Cracks and the Energy of Elastic Deformation," *Transactions*, American Society of Mechanical Engineers, 1958.

OISTRIBUTION LIST

No. of Copies	To
1	Office of the Director, Oefense Research and Engineering, The Pentagon, Washington, O. C. 20301
12	Commander, Oefense Documention Center, Cameron Station, Building 5, SOIO Ouke Street, Alexandria, Virginia 22314
1	Metals and Ceramics Information Center, Battelle Memorial Institute, SOS King Avenue, Columbus, Ohio 43201
	Chief of Research and Oevelopment, Department of the Army, Washington, O. C. 20310
2	ATTN: Physical and Engineering Sciences Oivision
	Commander, Army Research Office, P.O. Box 12211, Research Triangle Park, North Carolina 27709
1	ATTN: Information Processing Office
	Commander, U. S. Army Materiel Oevelopment and Readiness Command, SOOI Eisenhower Avenue, Alexandria, Virginia 22333
1	ATTN: DRCOE-L, Light Armor Coordination Office
1	ORCOE-TC
1	ORCSA-S, Or. R. B. Oillaway, Chief Scientist
	Commander U. S. Army Electronics Command, Fort Monmouth, New Jersey 07703
1	ATTN: AMSEL-GG-OO
1	AMSEL-GG-OM
1	AMSEL-GG-E
1	AMSEL-GG-EA
1	AMSEL-GG-ES
1	AMSEL-GG-EG
1	Commander, U. S. Army Missile Command, Redstone Arsenal, Alabama 35809
1	ATTN: Technical Library
1	AMSMI-RSM, Mr. E. J. Wheelahan
	Commander, U. S. Army Natick Laboratories, Natick, Massachusetts 01760
1	ATTN: Technical Library
1	Or. E. W. Ross
1	STSNL-AAP, Mr. J. Falcone
	Commander, U. S. Army Satellite Communications Agency, Fort Monmouth, New Jersey 07703
1	ATTN: Technical Document Center
	Commander, U. S. Army Tank-Automotive Command, Warren, Michigan 48090
1	ATTN: AMSTA-R
2	AMSTA, Research Library Branch
	Commander, U. S. Army Armament Command, Rock Island, Illinois 61201
2	ATTN: Technical Library
	Commander, White Sands Missile Range, New Mexico 88002
1	ATTN: STEWS-WS-VT
	Commander, Aberdeen Proving Ground, Maryland 2100S
1	ATTN: STEAP-TL, Bldg. 30S
	Commander, Edgewood Arsenal, Maryland 21010
1	ATTN: Mr. F. E. Thompson, Oir. of Eng. & Ind. Serv., Chem-Mun Br
	Commander, Frankford Arsenal, Philadelphia, Pennsylvania 19137
1	ATTN: Library, H1300, Bl. S1-2
1	SMUFA-L300, Mr. J. Corrie
	Commander, U. S. Army Ballistic Research Laboratory, Aberdeen Proving Ground, Maryland 2100S
1	ATTN: Or. J. Frasier
1	Or. R. Vitali
1	Or. G. L. Filbey
1	Or. R. Karpp
1	Or. W. Gillich
	Commander, Harry Oiamond Laboratories, 2800 Powder Mill Road, Adelphi, Maryland 20783
1	ATTN: Technical Information Office
	Commander, Picatinny Arsenal, Dover, New Jersey 07801
1	ATTN: SMUPA-RT-S
1	Mr. A. Oevine
1	Mr. A. M. Anzalone, SARPA-FR-M-D, PLASTEC
	Commander, Redstone Scientific Information Center, U. S. Army Missile Command, Redstone Arsenal, Alabama 35809
4	ATTN: AMSMI-RBLO, Document Section
	Commander, Watervliet Arsenal, Watervliet, New York 12189
1	ATTN: SWEWV-ROT, Technical Information Services Office
1	Or. T. Oavidson
1	Mr. O. P. Kendall
1	Mr. J. F. Throop
1	SWEWV-ROR, Or. F. W. Schmiedeshoff
	Commander, U. S. Army Foreign Science and Technology Center, 220 7th Street, N. E., Charlottesville, Virginia 22901
1	ATTN: AMXST-SO3
	Commander, U. S. Army Aeromedical Research Unit, P. O. Box S77, Fort Rucker, Alabama 36460
1	ATTN: Technical Liorary
	Oirector, Eustis Oirectorate, U. S. Army Air Mobility Research and Oevelopment Laboratory, Fort Eustis, Virginia 23604
1	ATTN: Mr. J. Robinson, SAVOL-EU-SS
1	Mr. R. Berresford
	Librarian, U. S. Army Aviation School Library, Fort Rucker, Alabama 36360
1	ATTN: Building S907
	Commander, U. S. Army Board for Aviation Accident Research, Fort Rucker, Alabama 36360
1	ATTN: Library, Bldg. SSOS
	Commander, USACDC Air Oefense Agency, Fort Bliss, Texas 79916
1	ATTN: Technical Library
	Commander, U. S. Army Engineer School, Fort Belvoir, Virginia 22060
1	ATTN: Library
	Commander, U. S. Army Engineer Waterways Experiment Station, Vicksburg, Mississippi 39180
1	ATTN: Research Center Library
	Commander, U. S. Army Mobility Equipment Research and Oevelopment Center, Fort Belvoir, Virginia 22060
1	ATTN: SMEFB-MM, Materials Research Laboratory, Mr. William H. Baer
	Aeronautic Structures Laboratories, Naval Air Engineering Center, Philadelphia, Pennsylvania 19112
1	ATTN: Library
	Naval Air Oevelopment Center, Aero Materials Oepartment, Warminster, Pennsylvania 18974
1	ATTN: J. Viglione
	Naval Ship Research and Oevelopment Laboratory, Annapolis, Maryland 21402
1	ATTN: Or. H. P. Chu
1	M. R. Gross
	Naval Underwater Systems Center, New London, Connecticut 06320
1	ATTN: R. Kasper
	Naval Research Laboratory, Washington, O. C. 20375
1	ATTN: C. O. Beachem
1	Or. J. M. Krafft - Code 8430
	Chief of Naval Research, Arlington, Virginia 22217
1	ATTN: Code 471
	Naval Weapons Laboratory, Washington, O. C. 20390
1	ATTN: H. W. Romine
	Oirector, Structural Mechanics Research, Office of Naval Research, 800 North Quincy Street, Arlington, Virginia 22203
1	ATTN: Or. N. Perrone
1	Ship Structure Committee, Maritime Transportation Research Board, National Research Council, 2101 Constitution Avenue, N. W., Washington, O. C. 20418
	Air Force Materials Laboratory, Wright-Patterson Air Force Base, Ohio 45433
2	ATTN: AFML (MXE), E. Morrissey
1	AFML (LC)
1	AFML (LMO), O. M. Forney
1	AFML (LNC), T. J. Reinhart
1	AFML, Or. J. C. Halpin
1	AFML, (MBC), Mr. Stanley Schulman
1	Or. S. Tsai
1	Or. N. Pagano
	Air Force Flight Oynamics Laboratory, Wright-Patterson Air Force Base, Ohio 45433
1	ATTN: AFFOL (FBC), C. Wallace
1	AFFOL (FBCB), G. O. Sendeckyj
	National Aeronautics and Space Administration, Washington, O. C. 20546
1	ATTN: Mr. B. G. Achhammer
1	Mr. G. C. Oeutsch - Code RR-1
	National Aeronautics and Space Administration, Marshall Space Flight Center, Huntsville, Alabama 35812
1	ATTN: R-P&VE-M, R. J. Schwinghamer
1	S&E-ME-MM, Mr. W. A. Wilson, Building 4720
	National Aeronautics and Space Administration, Langley Research Center, Hampton, Virginia 23365
1	ATTN: Mr. H. F. Hardrath, Mail Stop 129
1	Mr. R. Foye, Mail Stop 1BBA

No. of Copies	To
	National Aeronautics and Space Administration, Lewis Research Center, 21000 Brook Park Road, Cleveland, Ohio 44135
1	ATTN: Mr. S. S. Manson
1	Dr. J. E. Srawley, Mail Stop 1DS-1
1	Mr. W. F. Brown, Jr.
	Panametrics, 221 Crescent Street, Waltham, Massachusetts 02154
1	ATTN: Mr. K. A. Fowler
	Wyman-Gordon Company, Worcester, Massachusetts 01601
1	ATTN: Technical Library
	Lockheed-Georgia Company, Marietta, Georgia 30063
1	ATTN: Advanced Composites Information Center, Dept. 72-14 - Zone 402
	Honeywell, Inc., Research Dept., S&RC, Mail Stop A3 34D, 2345 Walnut Street, Saint Paul, Minnesota 55113
1	ATTN: Mr. Gene Fisher
	National Bureau of Standards, U. S. Department of Commerce, Washington, D. C. 20234
1	ATTN: Mr. J. A. Bennett
1	Mr. W. F. Anderson, Atomics International, Canoga Park, California 91303
	Midwest Research Institute, 425 Coker Boulevard, Kansas City, Missouri 64110
1	ATTN: Mr. C. Q. Bowles
1	Mr. J. C. Grosskreutz
1	Mr. A. Hurlich, General Dynamics Convair, Mail Zone 572-00, P. O. Box 1128, San Diego, California 92112
	Virginia Polytechnic Institute and State University, Dept. of Engineering Mechanics, 230 Norris Hall, Blacksburg, Virginia 24061
1	ATTN: Prof. R. M. Barker
1	Assoc. Prof. G. W. Swift
	Southwest Research Institute, 8500 Culebra Road, San Antonio, Texas 78284
1	ATTN: Mr. G. C. Grimes
	IIT Research Institute, Chicago, Illinois 60616
1	ATTN: Dr. I. M. Daniel
1	Dr. R. E. Johnson, Mgr., Mechanics of Materials-AEG, Mail Drop M88, General Electric Company, Cincinnati, Ohio 45215
1	Mr. J. G. Kaufman, Alcoa Research Laboratories, New Kensington, Pennsylvania 15068
1	Mr. G. M. Orner, MANLABS, 21 Erie Street, Cambridge, Massachusetts 02139
1	Mr. P. N. Randall, TRW Systems Group - 0-1/2210, One Space Park, Redondo Beach, California 90278
	TRW Equipment, TRW Inc., 2355 Euclid Avenue, Cleveland, Ohio 44117
1	ATTN: Dr. E. A. Steigerwald, T/M-3296
1	Dr. I. S. Tuba, Basic Technology, Inc., 712 Saltsburg Road, Pittsburgh, Pennsylvania 15235
1	Mr. W. A. Van der Sluys, Research Center, Babcock and Wilcox, Alliance, Ohio 44601
1	Mr. B. M. Wundt, 2346 Shirl Lane, Schenectady, New York 12309
	Battelle Memorial Institute, 505 King Avenue, Columbus, Ohio 43201
1	ATTN: Dr. E. Rybicki
1	Dr. K. R. Merckx, Battelle Northwest Institute, Richland, Washington 99352
	General Electric Company, Schenectady, New York 12010
1	ATTN: Mr. A. J. Brothers, Materials and Processes Laboratory
	General Electric Company, Knolls Atomic Power Laboratory, P. O. Box 1072, Schenectady, New York 12301
1	ATTN: Mr. F. J. Mehringer
1	Mr. L. F. Coffin, General Electric Research Laboratory, P. O. Box 1088, Schenectady, New York 12301
	United States Steel Corporation, Monroeville, Pennsylvania 15146
1	ATTN: Dr. A. K. Shoemaker, Applied Research Laboratory
	Westinghouse Electric Company, Bettis Atomic Power Laboratory, P. O. Box 109, West Mifflin, Pennsylvania 15122
1	ATTN: Mr. M. L. Parrish

No. of Copies	To
	Westinghouse Electric Company, Pittsburgh, Pennsylvania 15235
1	ATTN: Mr. R. E. Peterson, Research Laboratories
1	Mr. E. T. Wessel, Research and Development Center
1	Mr. B. F. Langer, Westinghouse Nuclear Energy Systems, P. O. Box 355, Pittsburgh, Pennsylvania 15230
1	Mr. M. J. Manjoine, Westinghouse Research Laboratory, Churchill Boro, Pittsburgh, Pennsylvania 15235
	Brown University, Providence, Rhode Island 02912
1	ATTN: Prof. J. R. Rice
1	Prof. W. N. Findley, Division of Engineering, Box D
	Carnegie-Mellon University, Department of Mechanical Engineering, Schenley Park, Pittsburgh, Pennsylvania 15213
1	ATTN: Dr. J. L. Swedlow
1	Prof. J. Dvorak, Chemical Engineering Department, Duke University, Durham, North Carolina 27706
	George Washington University, School of Engineering and Applied Sciences, Washington, D. C. 20006
1	ATTN: Dr. H. Liebowitz
	Lehigh University, Bethlehem, Pennsylvania 18015
1	ATTN: Prof. George R. Irwin
1	Prof. G. C. Sih
1	Prof. F. Erodgan
	Massachusetts Institute of Technology, Cambridge, Massachusetts 02139
1	ATTN: Prof. T. H. H. Pian, Department of Aeronautics and Astronautics
1	Prof. F. J. McGarry
1	Prof. A. S. Argon, Room 1-312
1	Mr. William J. Walker, Air Force Office of Scientific Research, 1400 Wilson Boulevard, Arlington, Virginia 22209
1	Prof. R. Greif, Dept. of Mech. Eng., Tufts University, Medford, Massachusetts 02155
1	Dr. D. E. Johnson, AVCO Systems Division, Wilmington, Massachusetts 01887
1	Prof. B. Pipes, Dept. of Mech. Eng., Drexel University, Philadelphia, Pennsylvania 19104
1	Prof. A. Tetelman, Dept. of Materials Science, University of California, Los Angeles, California 90024
1	Prof. W. Goldsmith, Dept. of Mech. Eng., University of California, Berkeley, California 94700
1	Prof. A. J. McEvilly, University of Connecticut, Storrs, Connecticut 06268
1	Prof. D. Drucker, Dean of School of Engineering, University of Illinois, Champaign, Illinois 61820
	University of Illinois, Urbana, Illinois 61820
1	ATTN: Prof. H. T. Corten, Dept. of Theoretical and Applied Mechanics, 212 Talbot Laboratory
1	Dr. M. L. Williams, Dean of Engineering, 240 Benedum Hall, University of Pittsburgh, Pittsburgh, Pennsylvania 15261
1	Prof. A. Kobayashi, Dept. of Mechanical Engineering, University of Washington, Seattle, Washington 98105
1	Mr. W. A. Wood, Baillieu Laboratory, University of Melbourne, Melbourne, Australia
1	Mr. Elmer Wheeler, Airesearch Manufacturing Company, 402 S. 36th Street, Phoenix, Arizona 85034
1	Mr. Charles D. Roach, U.S. Army Scientific and Technical Information Team, 600D Frankfurt/Main, I.G. Hochhaus, Room 75D, West Germany (APO 09710, NY)
1	Prof. R. Jones, Dept. of Civil Eng., Ohio State University, 206 W 18th Avenue, Columbus, Ohio 43210
	State University of New York at Stony Brook, Stony Brook, New York 11790
1	ATTN: Prof. Fu-Pen Chiang, Dept. of Mechanics
	E. I. Du Pont de Nemours and Company, Wilmington, Delaware 19898
1	ATTN: Dr. Carl Zweren, Industrial Fibers Div., Textile Fibers Dept.
	Washington University, St. Louis, Missouri 63130
1	ATTN: Prof. E. M. Wu
	Director, Army Materials and Mechanics Research Center, Watertown, Massachusetts 02172
1	ATTN: DRXMR-PL
1	DRXMR-AG
2	Authors

Army Materials and Mechanics Research Center,
Watertown, Massachusetts 02172
FRACTURE OF COMPOSITE COMPACT
TENSION SPECIMENS -
John M. Slepetz and Leonard Carlson

Technical Report AMMRC TR 76-9, March 1976, 22 pp -
illus-tables, O/A Project 1T162105AH84,
AMCMS Code 612105.11.H8400

AD_____

UNCLASSIFIED
UNLIMITED DISTRIBUTION

Key Words

Composite materials
Fiber composites
Fracture (materials)

Fracture experiments were carried out on compact tensinn specimens of unidirectional and cross-ply S-glass/epoxy and graphite/epoxy. Fracture toughness values were determined by the compliance calibration technique and by measuring the area under the load-displacement curve. In unidirectional specimens, crack extension was always parallel to the fibers and was dependent on crack length. Toughness did not vary significantly with fiber orientation relative to the load direction in unidirectional S-glass/epoxy. Tests on cross-ply S-glass specimens were not valid because crack propagation did not occur; instead, a zone containing a system of superficial parallel cracks and other damage developed, which extended with increasing load. Cross-ply graphite specimens, on the other hand, did appear to give valid test results although the cracks propagated were not always straight and other damage mechanisms were also present. Toughness values for cross-ply graphite were approximately two orders of magnitude higher than for unidirectional specimens due chiefly to the fracture resistance of fibers transverse to the crack. Toughness values determined by the compliance calibration method were consistent with reported values obtained by other methods.

Army Materials and Mechanics Research Center,
Watertown, Massachusetts 02172
FRACTURE OF COMPOSITE COMPACT
TENSION SPECIMENS -
John M. Slepetz and Leonard Carlson

Technical Report AMMRC TR 76-9, March 1976, 22 pp -
illus-tables, O/A Project 1T162105AH84,
AMCMS Code 612105.11.H8400

AO_____

UNCLASSIFIED
UNLIMITED DISTRIBUTION

Key Words

Composite materials
Fiber composites
Fracture (materials)

Fracture experiments were carried out on compact tensinn specimens of unidirectional and cross-ply S-glass/epoxy and graphite/epoxy. Fracture toughness values were determined by the compliance calibration technique and by measuring the area under the load-displacement curve. In unidirectional specimens, crack extension was always parallel to the fibers and was dependent on crack length. Toughness did not vary significantly with fiber orientation relative to the load direction in unidirectional S-glass/epoxy. Tests on cross-ply S-glass specimens were not valid because crack propagation did not occur; instead, a zone containing a system of superficial parallel cracks and other damage developed, which extended with increasing load. Cross-ply graphite specimens, on the other hand, did appear to give valid test results although the cracks propagated were not always straight and other damage mechanisms were also present. Toughness values for cross-ply graphite were approximately two orders of magnitude higher than for unidirectional specimens due chiefly to the fracture resistance of fibers transverse to the crack. Toughness values determined by the compliance calibration method were consistent with reported values obtained by other methods.